communications earth & environment

ARTICLE

https://doi.org/10.1038/s43247-022-00372-2 OPEN

Radiation damage allows identification of truly inherited zircon

Anders Bjerga [1✉], Håvard Hallås Stubseid[1], Leif-Erik Rydland Pedersen[1] & Rolf Birger Pedersen[1]

Many studies have reported U-Pb dates of zircon that are older than the igneous rocks that contain them, and they are therefore thought to be inherited from older rock complexes. Their presence has profound geodynamic implications and has been used to hypothesize about concealed micro-continents, continental crust beneath ocean islands, and recycling of continental material in the mantle beneath mid-ocean ridges. Here, we combine single zircon U-Pb dates and structural radiation damage determined by Raman spectroscopy from a Pliocene mid-ocean ridge gabbro and from Cenozoic igneous rocks to test whether radiation damage allows distinction between contamination and truly inherited zircon. We find that Precambrian zircon found in the Pliocene sample has accumulated substantially more radiation damage than could be explained if they had truly been inherited. In the Cenozoic samples, however, we find that the radiation damage of old grains corresponds with that of young magmatic zircon, suggesting they are genuinely inherited.

[1] Center for Deep Sea Research and Department of Earth Science, University of Bergen, Allégaten 41, 5007 Bergen, Norway.
✉email: anders.bjerga@gmail.com

Inherited zircon ($ZrSiO_4$), displaying U–Pb dates older than their host-rock, are a common feature of felsic rocks and are increasingly being reported from mafic and ultramafic rocks from both oceanic[1–7] and continental[8–14] settings. While the ability to inherit older zircon in continental settings remains indisputable, reports suggesting that zircon can survive and retain the U–Pb dates under certain chemical conditions in the mantle[9,15,16] indicate that zircon may be recycled through the mantle, and therefore appear in mantle peridotites or mantle-derived igneous rocks. However, experimental studies show that zircon undergoes rapid dissolution in mafic melts raising questions about the true origin of zircon in these settings[17–20]. During investigations of a Pliocene gabbro sampled from a peridotite-gabbro complex in the Mohns ridge (Fig. 1), we recovered several grains of zircon using conventional mineral separation (see "Methods" section for details). For zircon produced by the gabbroic magma, we expected dates between 3 and 5 Ma, consistent with magnetic anomalies and seafloor spreading rates. For some of these grains, Precambrian dates were obtained, significantly older than anticipated, with the oldest grain having a $^{207}Pb/^{206}Pb$ date of 2724 Ma. If these zircon grains are derived from recycled continental material in the sub-oceanic mantle source of the peridotite-gabbro complex, it clearly has significant geodynamic implications.

Because the risk of contamination during sample handling and preparation will always be a concern, methods for verifying the true origin of zircon grains are crucial, especially in samples with low zircon yields. Low-temperature thermochronological methods, such as fission tracks and (U–Th)/He, may shed light on the most recent thermal history of zircon[9,21–25]. Unfortunately, these methods are time-consuming, destructive, and require crystals of a certain quality and size to get proper age determinations. An alternative method involves Raman spectroscopy, which allows for in situ (~2 µm spatial resolution) characterization of the radiation damage to the zircon lattice[26–31]. Experiments have shown that moderately radiation-damaged zircon reorganizes their structure at >700 °C on a timescale of hours to days[26,32,33]. This implies that zircon grains incorporated in a melt will anneal and show similar crystallinity to the zircon that crystallized with the host rock, while the original U–Pb dates may be preserved due to low Pb-diffusion rates[15].

Because of the widespread geodynamic implications of inherited zircon in oceanic igneous rocks, and the possibility for misinterpretation of contaminated grains as inherited, this paper aims to show how radiation damage measured through rapid and non-destructive Raman spectroscopy may remove uncertainties regarding sample contamination. Importantly, this approach can be used to revisit previously investigated samples to verify the findings. We first present a study of zircon U–Pb dates and Raman spectroscopy analysis from a Pliocene ocean-ridge gabbro (Case 1, Mohns Ridge, 73°N: Fig. 1), and then we assess the method using a systematic study of magmatic and inherited zircon from igneous rocks that formed during the opening of the North-Atlantic Ocean (Case 2, Gjallar Ridge, 65°N: Fig. 1).

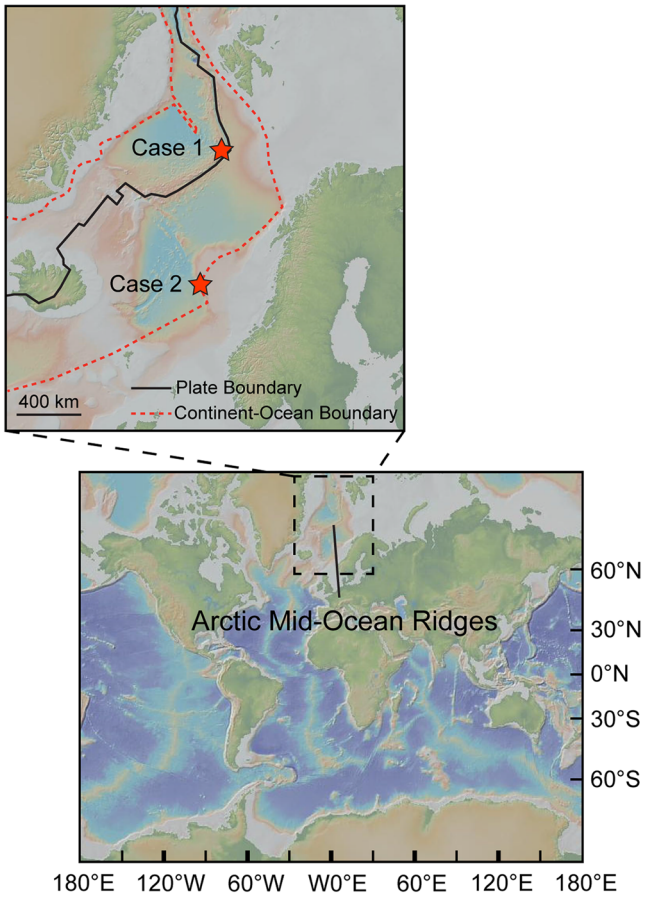

Fig. 1 Geographic overview over the study area. Case 1 is a Pliocene mid-ocean ridge gabbro while Case 2 is Cenozoic dacitic-tracydacitic sills that intruded Cretaceous sedimentary rocks. The black line and red dotted lines represent the plate boundary and the continent-ocean boundary, respectively. Maps were created using GeoMapApp (www.geomapapp.org).

Results and discussion

Case 1: Precambrian zircon in mid-ocean ridge gabbro. A single ocean-ridge gabbro sample (GS16A-ROV6-016: Case 1: Fig. 1) was selected for zircon separation using ~10 kg of material. Based on a Raman spectroscopy screening before mounting of zircon grains in epoxy, 18 grains out of 44 recovered were selected for U–Pb isotope analysis using LA-ICP-MS. One grain (GS16A-ROV06-16-11-3) had too low Pb content to yield a reliable age. Seven grains yield Pliocene U–Pb systematics with a mean weighted average $^{206}Pb/^{238}U$ age of 4.15 ± 0.13 Ma (MSWD = 1.2, $n = 7$) and has a characteristic low U (between 8 and 64 ppm) and Th content (between 7 and 72 ppm) and effective U concentrations ($eU = U + 0.235$ Th) between 10 and 81 ppm (Supplementary Data 1). One analysis on grain GS16A-ROV06-16-02-3 shows markedly high U (606 ppm) and Th (711 ppm) yielding an effective U concentration of 773 ppm. The grains are subhedral to euhedral and exhibit concentric and oscillatory zoning in cathodoluminescence images (Fig. 2), indicating that the grains have crystallized from a melt. They show mean ν3 (SiO_4) peak position of 1008.8 cm^{-1} and a range from 1008.0 to 1009.6 cm^{-1}. The full width at half maximum (FWHM), corrected for spectral resolution, shows a mean of 3.1 and a range between 2.6 and 3.5 (Fig. 3a and Supplementary Data 2). Ten grains with both oscillatory and sector zoning (Fig. 2) have Precambrian U–Pb dates, with individual spot analysis yielding U–Pb dates that range from 2724 to 554 Ma (Supplementary Data 1). They have variable U (between 82 and 541 ppm) and Th (between 53 and 396 ppm) concentrations and show a linear shift of ν3 (SiO_4) peak positions consistent with the accumulation of radiation damage because of alpha-decay (Fig. 3a). Internal radiation doses were calculated for the Precambrian zircon (details in "Methods" section) and plot below the expected trajectory for unannealed grains (Fig. 3b).

We interpret the mean $^{206}Pb/^{238}U$ age of 4.15 ± 0.13 Ma to represent the crystallization of the mafic magma during plate separation, which is consistent with the sample position relative to

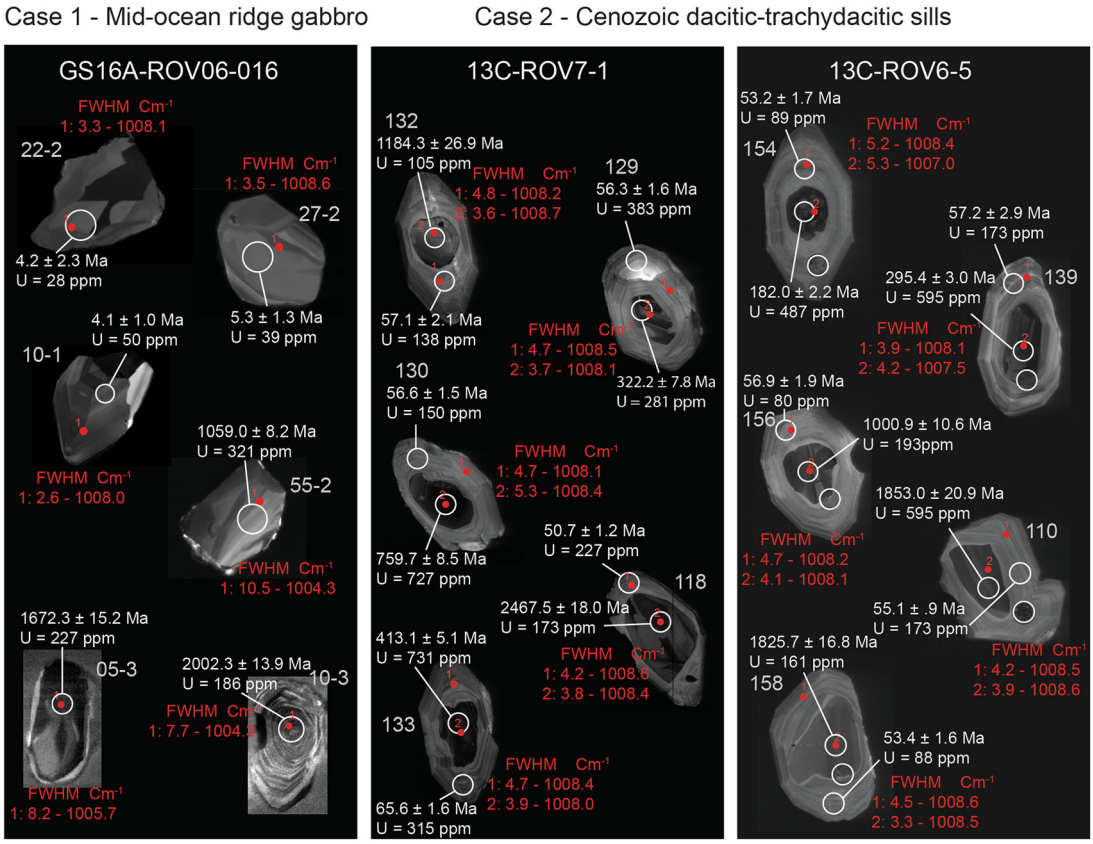

Fig. 2 Representative cathodoluminescence images of zircon grains. White circles correspond to 26 µm laser-ablation spots. Circles that have no associated value are analyses that are not reported or used in this study.

the rift valley. The unexpected presence of Precambrian zircon in the young oceanic lithosphere requires a careful appraisal. A possible explanation is that these grains were recycled from older crustal rocks in the mantle source[1,3]. Earlier reports of inherited zircon in mantle-derived rocks often assumed that their studied grains belonged to that specific sample, however, U–Pb dates alone do not rule out other explanations. Another plausible explanation is that they are contaminants from sample processing. Experiments have shown that moderately radiation-damaged zircon completely reorganizes their structure at 900 °C at timescales of hours to days[32]. Consequently, grains that were incorporated into a mafic melt should show crystallinities similar to the young magmatic grains even if they occurred as inclusions in major mineral phases or within xenoliths[21]. The large spread in zircon ν3 (SiO_4) peak positions ranging from 1007.8 to 998.0 cm^{-1} and FWHM between 4.4 and 14.9 (Fig. 3a, b and Supplementary Data 2) show that the older-than host rock grains have accumulated substantially more radiation damage than they would have if they had been annealed at ~5 Ma. The observations and data presented here demonstrate that the Precambrian zircon grains are contaminated from sample processing and not truly inherited zircon.

Case 2: Older-than host rock zircon in Cenozoic sills. To confirm that our approach allows distinction between contamination during sample preparation and truly inherited zircon, we tested the Raman systematics in dacitic-trachydacitic sills that intruded Cretaceous sedimentary rocks during the opening of the North-Atlantic Ocean (samples 13C-ROV6-5 and 13C-ROV6-71: Case 2: Fig. 1), and are therefore likely to contain inherited zircon of continental origin. A total of 215 grains were analyzed for U–Pb by LA-ICP-MS, in grains where it was possible, both rims and interior sections were analyzed to compare internal age differences resulting in 448 analytical spots (Supplementary Data 1). Zircon grains are morphologically similar, showing well-developed oscillatory zoning with occasional grains displaying sector zoning. The two analyzed samples yielded mean weighted average $^{206}Pb/^{238}U$ ages of 54.21 ± 0.13 Ma (MSWD = 2.16; $n = 46$) and 55.57 ± 0.12 Ma (MSWD = 4.14; $n = 63$), analysis with over 2% uncertainty or discordance were excluded from the age calculations. This is within the uncertainty of previously reported weighted mean TIMS U–Pb ages of magmatic sills in the Vøring basin[34]. Seventy-nine analyses from oscillatory zoned rims and rounded to subhedral cores displaying oscillatory, sector, or mottle zoning textures (Fig. 2) yield dates between 80 and 2200 Ma (Supplementary Data 1). Rim thickness range from less than a couple of µm to more than 50 µm. Uranium concentrations obtained from the same zircon volume dated by LA-ICP-MS show mean and median concentrations of 187 ppm and 151 ppm, respectively, and a range in U content from 12 to 1430 ppm. The concentration of Th ranges from 5 to 759 ppm and U/Th has a mean of 3.4 and a median of 3.3. The effective U concentration ranges from 55 to 857 ppm with a mean and median of 203 ppm and 172 ppm, respectively.

We studied 87 of the dated grains, both young magmatic and old inherited, by using Raman spectroscopy to investigate the effect of structural recovery of zircon included in the melt (all data is available in Supplementary Data 2). In 37 composite grains, we analyzed both rim and core leading to a total of 116 measurements. Grains are atomically well-ordered with a mean ν3 (SiO_4) peak position of 1008.2 cm^{-1} and a range from 1006.5 to 1009.2 cm^{-1}. The full width at half maximum (FWHM), corrected for spectral resolution, shows a mean of 4.3, a median of 4.2, and a range between 3.2 and 6.0 (Fig. 3c). Cores generally display lower ν3 (SiO_4) peak positions and higher eU compared with rims (Fig. 2).

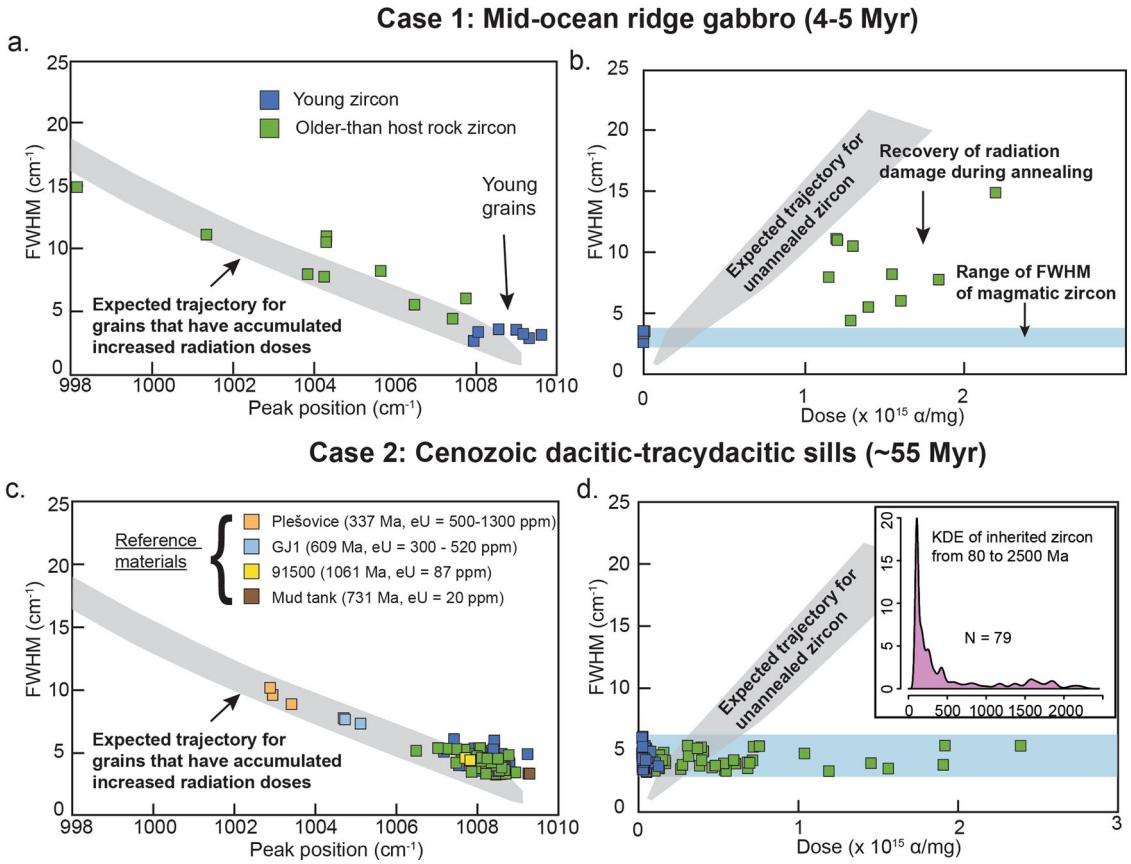

Fig. 3 Evaluation of radiation damage of single zircon grains. a, **c** The full width at half maximum (FWHM) vs. peak position of the ν3 (SiO_4) stretching band. The expected trajectory for grains that have accumulated increased radiation doses is from Geisler et al.[30]. **b**, **d** FWHM vs. α-dose for young and inherited zircon grains. Data for unannealed zircon from Nasdala[28]. The vertical axis on the inset in **d** is based on histograms with a bandwidth of 40 Ma. Note that the young and old zircon grains in case 1 (mid-ocean ridge gabbro) plot at different locations in FWHM vs. peak position space while both young and older zircon in case 2 (Cenozoic sills) overlap.

The tight clustering of the zircon ν3 (SiO_4) peak positions at ~1008 cm^{-1} and FWHM of ~4.0 show that the inherited grains have crystallinities comparable to the young magmatic zircon (Fig. 3c). Most internal radiation doses calculated for the old inherited zircon (see "Methods" section) plot below a calibration curve for unannealed grains (Fig. 3d) demonstrating that they have experienced annealing of the radiation damage after their formation. The calculated radiation doses using U and Th concentrations for the young zircon grains exceed what can be ascribed to internal radiation doses purely by α-decay (i.e., they plot above the trajectory for unannealed zircon in Fig. 3d), suggesting internal tensional strain due to substitution or rapid growth[35,36].

Our finding of older-than host rock zircon in Cenozoic dacitic-trachydacitic sills with crystallinity similar to the young magmatic grains (Fig. 3c, d) demonstrates that the grains share the same recent thermal history. The range of observed FWHM fits remarkably well with the expected range for the accumulation of radiation damage since approximately 55 Ma at a range of eU content from ~200 to 1500 ppm (Fig. 4). In contrast, older grains that did not experience this annealing event would have accumulated radiation damage for longer periods and should show higher FWHM (i.e., following the trajectory in Fig. 3c, d). As in the case of mid-ocean ridge gabbro (Case 1), such grains should therefore be considered foreign to the sample. We

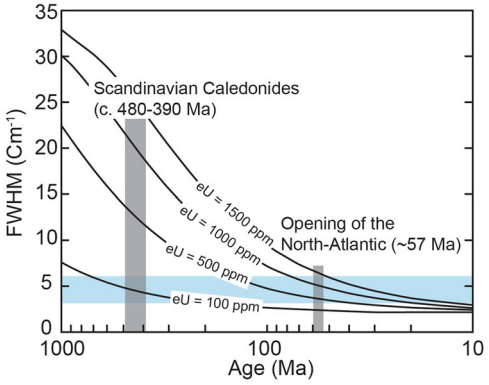

Fig. 4 Calculated radiation damage of single zircon grains as a function of time and eU. Evolution of radiation damage, measured as FWHM, through time of single zircon grains at different eU-content. The blue band shows the range of observed FWHM of both young magmatic and old inherited zircon from case 2. The expected FWHM for zircon grains formed or annealed during the opening of the North-Atlantic (~57 Ma) and the Caledonian orogen (c. 480–390 Ma) is shown as gray boxes for reference. Details about the calculations of the contour lines (radiation damage ages) are found in the "Methods" section.

find that inherited grains yield radiation damage close to the magmatic age (Figs. 3c and 4), demonstrating the promise of this approach for the identification of inherited zircon.

Implications for the interpretation of inherited zircon. The presence of continental zircon in oceanic rocks has long been considered an enigmatic feature owing to the sparse evidence of their actual origin. Because current practices for the identification of inherited zircon are based primarily on U–Pb dates, it is hampered because grains having old cores with rim dates similar to host-rock are rare. Luminescence features and trace element composition of zircon are process-dependent, meaning that zircon coming from potential microcontinents or incorporated continental material will significantly overlap with those from the continent, making them less useful as indicators for inheritance. Our demonstration that the annealing of zircon in natural magmas may provide evidence for the existence of inherited materials is significant in at least two major respects. First, it provides a framework for the identification and interpretation of inherited zircon in a range of geological settings, such as mid-ocean ridges[1,3], oceanic hot spots[4,5], and island arcs[37,38]. This approach is especially suited for young magmatic rocks, where the age contrast between inherited and magmatic zircon may be large. Second, the method provides a means to revisit previously dated samples, potentially leading to the verification of disputed hypotheses. Implementation of this approach will improve our understanding of crustal recycling in the mantle and continental-influenced magmatism by removing uncertainty related to the true origin of inherited material, and may lead to a re-evaluation of current geodynamic models. An important difference may be made concerning continental rocks, which commonly have more complex histories compared to oceanic rocks. For instance, in a study of inherited zircon in kimberlites, Nasdala[39] found negligible annealing and interpreted this to reflect that zircon must have been residing in the lower crust and trapped in melts where they experienced low temperatures (<800 °C) and/or rapid cooling (on the order of hours to days). Consequently, because zircon annealing depends on both time and temperature, there may be cases where the applied methodology might not be as straightforward and require a careful appraisal of the specific geodynamic context. Capturing the full suite of variables and parameters that might affect zircon annealing will require additional systematic studies of zircon inheritance in samples with well-constrained histories. Figure 4 shows that at low eU concentrations, the FWHM of zircon evolves slowly (shallow slope), and relatively high uncertainties (typically <20%) in the concentrations of U and Th and the Raman data may lead to situations where the radiation damage age of individual grains becomes unreliable. At higher eU concentrations, however, the slopes in Fig. 4 become steeper which should allow for more precise age constraints.

The fact that we did not find inherited zircon which would indicate the presence of continental material in the shallow upper mantle beneath the Mohns Ridge has implications for understanding the mantle dynamics, and warrants a discussion on why inherited zircon that appear elsewhere along the ridge segment are lacking here. Three contrasting possibilities must be evaluated: (1) recycling of continental material is localized to distinct regions of the mid-ocean ridges; (2) incorporation of continental material occurs at variable rates through time; (3) earlier proposed inherited zircon represents contamination due to sample preparation. Considering that old inherited zircon has been reported from several locations in the Mid-Atlantic Ridge, such strong localization of continental material along the mid-ocean ridge appears unlikely. In addition, the slow-spreading rate, proximity to the continental margin, and young age of the Norwegian-Greenland Sea are factors that should increase the likelihood of discovering a continental signature. It is possible that the recycling of continental material in the oceanic mantle asthenosphere is less widespread than previously proposed and occurs in discrete pulses, but there are currently too few constraints to draw any firm conclusions. An alternative explanation is that previously proposed inherited grains are derived from contamination by grains from another sample during laboratory preparation. Despite taking all precautions possible during sample processing, there will always be the possibility that contamination may occur. Previous reports of inherited zircon along the mid-ocean ridge have focused on U–Pb dating of separated zircon grains, and in situ studies have been unable to replicate the findings[40,41]. Failure to address the low-temperature history of the grains and a lack of in situ confirmation, therefore, leaves significant uncertainty related to the interpretation of inherited zircon in the sub-oceanic mantle and beneath ocean islands. Consequently, the results from the two-step approach presented here raise intriguing questions regarding the nature and extent of continental recycling along the mid-ocean ridges, which may be resolved by careful consideration of the thermal history of individual grains of zircon.

Methods

Sample descriptions. Oceanic gabbro sample GS16A-ROV6-016 from case 1 was collected using a remotely operated vehicle during a research cruise with G/O SARS in 2016 at a depth of 2449 mbsl at the Schulz Massif (73.7298N 7.5191E, Fig. 1). The rock is undeformed and comprises large plagioclase and pyroxene crystals, which have been affected by various degrees of hydrothermal alteration. The subhedral to euhedral zircon grains have a mean length of 112 µm, a median length of 101 µm, and a range between 53 and 230 µm. Sector zoning and oscillatory zoning are visible in cathodoluminescence images (CL) and are interpreted to represent growth textures as the minerals crystallized from magma.

Dacite (13C-ROV6-5: 65.8958N 1.7944E) and trachydacite (13C-ROV7-1: 65.8979N 1.7846E) were sampled during a research cruise with the M/V Seabed Worker in 2013 at depths of 2205 mbsl and 2755 mbsl, respectively, at the Gjallar Ridge (Case 2: Fig. 1). In the thin section, zircon occurs within feldspar and garnet phenocrysts, and as free crystals within the fine-grained matrix. Zircon, quartz, apatite, monazite, and FeTi-oxides are found as inclusions in garnet. The zircon grains are euhedral to subhedral, have a mean length of 216 µm, a median length of 170 µm, a mode of 119 µm, and range between 61 and 820 µm. Sector zoning and oscillatory zoning are visible in cathodoluminescence images (CL). Several grains display core-rim morphology and have characteristic rounded cores, which are both darker and lighter than their rim in CL images. No resorption or micro-porosity, which indicates alteration, was observed.

U-Pb geochronology. Approximately 10 kg of gabbro and 2–3 kg of dacite/trachydacite were crushed by hand and put through a Wifley-shaking table, after which the magnetic minerals were removed using a Frantz magnetic separator. The remaining material was run through a single heavy liquid step using diiodomethane to concentrate zircon. Grains were hand-picked and mounted in 25 mm epoxy blocks and polished to expose the zircon for further analysis. Mounts were then imaged in transmitted and reflected light using a Nikon LV100Pol polarizing microscope with a DS-Fi3 color camera, followed by backscatter and cathodoluminescence conducted using a Zeiss Supra 55VP SEM at the University of Bergen. Zircon parameters were measured using thresholding and particle counting in ImageJ.

U–Pb analysis of zircon grains was performed at Bergen Geoanalytical Facility at the University of Bergen using a 193 nm ArF excimer laser ablation system (RESOlution M-50 LR) coupled to an HR-SC-ICP-MS (Nu Instruments Attom ES) using parameters reported in Supplementary Table 1. The zircon grains were ablated for 30 s, after 15 s of blank measurement, using a 26 µm spot size, 5 Hz, and a fluence between 2 and 2.5 J/cm^2. The data were acquired in time-resolved peak-jumping pulse-counting mode with 1 point measured per peak for masses ^{202}Hg + ^{204}Pb + Hg, ^{206}Pb, ^{207}Pb, ^{208}Pb, ^{232}Th, ^{235}U, and ^{238}U. Because of the non-linear transition between the two counting modes in the ICP-MS, ^{238}U was calculated from ^{235}U when measured in attenuated mode (^{238}U counts = ^{235}U counts × 137.818) using a purpose-made python script.

Data reduction was done using Iolite 4 (v. 4.4.5) with the VizualAge UComPbine[42] data reduction scheme. In some grains, the ages increased with depth suggesting that different parts of the grain were ablated yielding mixed ages. In these cases, we integrated the data over the stable signal to reduce the possibility of mixed ages. Data reduction methodology follows Paton[43] and includes a correction for gas blank, laser-induced elemental fractionation of Pb and U, and instrument mass bias. Both blank counts and instrumental bias were corrected with

an automatic spline function, while down-hole element fractionation was corrected using an exponential or exponential + line function. Common Pb correction was not applied to the data, only monitored. The remaining element fractionation and instrumental mass bias were corrected by normalization to the natural zircon reference material 91500[44]. For quality control, the zircon reference materials GJ1[45], Plešovice[46], and Mud Tank[47] were measured regularly and values are reported in Supplementary Table 1. The uncertainty of the U and Th concentrations reported in Supplementary Data 1 and 2 is estimated to be <20%[47]. The IsoplotR[48] program was used to generate weighted average and kernel density estimate (KDE) plots. Uncertainties in the weighted average ages are reported as standard error (SE).

Measuring and evaluating zircon radiation damage in zircon. Raman spectra were recorded with a Jobin Yvon Labram-HR system equipped with an Olympus BX41 microscope, a Peltier-cooled charge-coupled device (CCD) detector, and 1800 grooves/mm diffraction grating. Excitation was performed using a 514 nm Ar-ion laser with absolute laser power of 15–20 mW through a density filter ($D = 0.3$) yielding a laser power of c. 7–10 mW on the sample surface. Measurements were made using a 50× objective. Wavenumber calibration was performed on the 520.7 cm^{-1} band of a silicon wafer and the Rayleigh line. Background subtraction and peak fitting were done with the Fityk 1.3.1 program[49]. Peaks were fitted with a PseudoVoigt function, and the peak shift position and width were determined for the ν3 (SiO_4) band at 1008 cm^{-1}. Bandwidth was corrected using the empirical correction formula of Váczi[50]:

$$\mathrm{FWHM_{true}} \approx \mathrm{FWHM_{meas}} - \frac{\mathrm{FWHM_{IPF}}^2}{0.9\mathrm{FWHM_{meas}} + 0.1\mathrm{FWHM_{IPF}}}, \quad (1)$$

where $\mathrm{FWHM_{IPF}}$ is the instrumental profile function.

Radiation damage to the zircon lattice is evaluated by measuring the full-width half maximum (FWHM) of the ν3 (SiO_4) peak position, which is a proxy for radiation damage. Crystals that have accumulated higher radiation doses (a factor of accumulation time and concentration of actinides) will have wider peaks with peak center position progressively lowered. By determining the U–Pb date, U and Th concentrations of a single zircon, we can calculate the α-dose received by that grain according to[28,51]:

$$D_\alpha = 8\times \frac{C_\mathrm{U}\times N_\mathrm{A}\times 0.9928}{M_{238}\times 10^6}\times\left(e^{\lambda_{238}t}-1\right) + 7\times \frac{C_\mathrm{U}\times N_\mathrm{A}\times 0.0072}{M_{235}\times 10^6}\times\left(e^{\lambda_{235}t}-1\right) + 6\times \frac{C_\mathrm{Th}\times N_\mathrm{A}}{M_{232}\times 10^6}\times\left(e^{\lambda_{232}t}-1\right), \quad (2)$$

where C_U and C_Th are the concentration of U and Th (in ppm), N_A is Avogadro's number (6.022×10^{23}), M_{238}, M_{235}, and M_{232} are the molecular weight of the isotopes, λ_{238}, λ_{235}, and λ_{232} are the respective decay constants, and t is the time. Decay constants for ^{238}U, ^{235}U and ^{232}Th are 1.55125×10^{-10}, 0.98485×10^{-9}, and 4.9475×10^{-11}, respectively.

A model calibration curve of unannealed zircon grains[28] allows us to calculate the zircon radiation damage age, which is the time required for that particular zircon to develop specific radiation damage[27,52]. The equation[27]:

$$\mathrm{FWHM} = A\left[1-\exp^{\left(-B_{\mathrm{FWHM}}D_{\mathrm{ed}}\right)}\right], \quad (3)$$

rearranged to:

$$D = \frac{\ln\left(1-\frac{\mathrm{FWHM}}{A}\right)}{-B}, \quad (4)$$

by Palenik[27] yields the damage dose (D) required to generate the observed radiation damage (given by the FWHM). A is the asymptotically approached FWHM value of 35.64. B is related to the mass of material damaged per α-decay event calculated as 5.32×10^{-19}/g. From this dose, the radiation damage age can be determined from the dose calculated using the U and Th concentrations in Eq. 2. Equations 3 and 4, which is based on the curve fitting of Raman data by Palenik[27], is slightly inaccurate because the model curve starts as 0 cm^{-1} Raman FWHM at zero damage[53]. A refined calibration by Váczi[53] which is on the form:

$$\mathrm{FWHM} = A_1 - A_2 e^{-\mathrm{BD}}, \quad (5)$$

was therefore used to calculate the evolution of FWHM at different eU shown in Fig. 4. In a recent study, Härtel[35] found an intercept of ~2.8 FWHM suggesting that compositional and/or structural differences impact the Raman bandwidth, which will have implications for the age estimates. In doing these calculations several assumptions and simplifications are made (see for instance the recent discussion in Härtel[35]). First, we assume that the U and Th concentrations and FWHM values are representative of the whole zircon grain or the studied section. However, zircon is commonly zoned with respect to radiation damage and trace element contents. Second, the spot size of LA-ICP-MS analysis is commonly ~26 µm wide and several µm deep, while Raman analysis has a spot size of <2–3 µm meaning that individual analysis may record variations that are due to local (horizontal or vertical) variations in the U–Th concentrations on scales <25 µm. Despite these uncertainties, reported radiation damage ages show geologically meaningful ages[54] and a similar age range as other low-temperature thermochronological methods, such as zircon and apatite (U/Th)/He[31,55]. The main difference is a consistent slightly older age determined by the radiation damage age method.

Data availability

All data generated or analyzed during this study are included in this published article (and its supplementary information files). In addition, all data have been uploaded to the Zenodo repository[56], available under https://doi.org/10.5281/zenodo.5937936.

Received: 3 August 2021; Accepted: 2 February 2022;
Published online: 23 February 2022

References

1. Pilot, J., Werner, C.-D., Haubrich, F. & Baumann, N. Palaeozoic and proterozoic zircons from the mid-Atlantic ridge. *Nature* **393**, 676–679 (1998).
2. Skolotnev, S. G., Bel'tenev, V. E., Lepekhina, E. N. & Ipat'eva, I. S. Younger and older zircons from rocks of the oceanic lithosphere in the Central Atlantic and their geotectonic implications. *Geotectonics* **44**, 462–492 (2010).
3. Bea, F. et al. Zircon xenocryst evidence for crustal recycling at the mid-Atlantic ridge. *Lithos* **354-355**, 1–11 (2020).
4. Ashwal, L. D., Wiedenbeck, M. & Torsvik, T. H. Archaean zircons in Miocene oceanic hotspot rocks establish ancient continental crust beneath Mauritius. *Nat. Commun.* **8**, 14086 (2017).
5. Torsvik, T. H. et al. A Precambrian microcontinent in the Indian Ocean. *Nat. Geosci.* **6**, 223–227 (2013).
6. Cheng, H. et al. Jurassic zircons from the Southwest Indian ridge. *Sci. Rep.* **6**, 26260 (2016).
7. Shellnutt, J. G., Lee, T.-Y., Chiu, H.-Y., Lee, Y.-H. & Wong, J. Evidence of middle Jurassic magmatism within the Seychelles microcontinent: Implications for the breakup of Gondwana. *Geophys. Res. Lett.* **42**, 207–210,215 (2015).
8. Xu, Z., Zheng, Y.-F. & Zhao, Z.-F. Zircon evidence for incorporation of terrigenous sediments into the magma source of continental basalts. *Sci. Rep.* **8**, 178 (2018).
9. Siebel, W. et al. Prolonged mantle residence of zircon xenocrysts from the western Eger rift. *Nat. Geosci.* **2**, 886–890 (2009).
10. Zhang, H.-F. et al. Phanerozoic reactivation of the Archean North China Craton through episodic magmatism: evidence from zircon U–Pb geochronology and Hf isotopes from the Liaodong Peninsula. *Gondwana Res.* **19**, 446–459 (2011).
11. Liu, Y. et al. Continental and Oceanic crust recycling-induced melt–peridotite interactions in the trans-North China Orogen: U–Pb dating, Hf isotopes and trace elements in zircons from mantle xenoliths. *J. Petrol.* **51**, 537–571 (2009).
12. Gao, S. et al. Recycling lower continental crust in the North China craton. *Nature* **432**, 892–897 (2004).
13. Robinson, P. T. et al. The origin and significance of crustal minerals in ophiolitic chromitites and peridotites. *Gondwana Res.* **27**, 486–506 (2015).
14. Yamamoto, S. et al. Recycled crustal zircons from podiform chromitites in the Luobusa ophiolite, southern Tibet. *Island Arc* **22**, 89–103 (2013).
15. Bea, F., Montero, P. & Palma, J. F. M. Experimental evidence for the preservation of U-Pb isotope ratios in mantle-recycled crustal zircon grains. *Sci. Rep.* **8**, 12904 (2018).
16. Kinny, P. D. & Meyer, H. O. A. Zircon from the mantle: a new way to date old diamonds. *J. Geol.* **102**, 475–481 (1994).
17. Borisova, A. Y. et al. Zircon survival in shallow asthenosphere and deep lithosphere. *Am. Mineral.* **105**, 1662–1671 (2020).
18. Dickinson, J. E. & Hess, P. C. Zircon saturation in lunar basalts and granites. *Earth Planet. Sci. Lett.* **57**, 336–344 (1982).
19. Borisov, A. & Aranovich, L. Zircon solubility in silicate melts: new experiments and probability of zircon crystallization in deeply evolved basic melts. *Chem. Geol.* **510**, 103–112 (2019).
20. Boehnke, P., Watson, E. B., Trail, D., Harrison, T. M. & Schmitt, A. K. Zircon saturation re-revisited. *Chem. Geol.* **351**, 324–334 (2013).
21. Blondes, M. S., Reiners, P. W., Edwards, B. R. & Biscontini, A. Dating young basalt eruptions by (U-Th)/He on xenolithic zircons. *Geology* **35**, 17–20 (2007).
22. Sutherland, F. L. & Fanning, C. M. Gem-bearing basaltic volcanism, Barrington, New South Wales: cenozoic evolution, based on basalt K–Ar ages and zircon fission track and U–Pb isotope dating. *Aust. J. Earth Sci.* **48**, 221–237 (2001).
23. Orme, D. A., Reiners, P. W., Hourigan, J. K. & Carrapa, B. Effects of inherited cores and magmatic overgrowths on zircon (U-Th)/He ages and age-eU trends from Greater Himalayan sequence rocks, Mount Everest region, Tibet. *Geochem. Geophys. Geosyst.* **16**, 2499–2507 (2015).

24. Guenthner, W. R., Reiners, P. W., Ketcham, R. A., Nasdala, L. & Giester, G. Helium diffusion in natural zircon: radiation damage, anisotropy, and the interpretation of zircon (U-Th)/He thermochronology. *Am. J. Sci.* **313**, 145–198 (2013).
25. Nasdala, L. et al. Incomplete retention of radiation damage in zircon from Sri Lanka. *Am. Mineral.* **89**, 219–231 (2004).
26. Ginster, U., Reiners, P. W., Nasdala, L. & Chanmuang, N. C. Annealing kinetics of radiation damage in zircon. *Geochim. Cosmochim. Acta* **249**, 225–246 (2019).
27. Palenik, C. S., Nasdala, L. & Ewing, R. C. Radiation damage in zircon. *Am. Mineral.* **88**, 770–781 (2003).
28. Nasdala, L. et al. Metamictisation of natural zircon: accumulation versus thermal annealing of radioactivity-induced damage. *Contrib. Mineral. Petrol.* **141**, 125–144 (2001).
29. Nasdala, L., Irmer, G. & Wolf, D. The degree of metamictization in zircon; a Raman spectroscopic study. *Eur. J. Mineral.* **7**, 471–478 (1995).
30. Geisler, T., Pidgeon, R. T., Van Bronswijk, W. & Pleysier, R. Kinetics of thermal recovery and recrystallization of partially metamict zircon: a Raman spectroscopic study. *Eur. J. Mineral.* **13**, 1163–1176 (2001).
31. Härtel, B., Jonckheere, R., Wauschkuhn, B. & Ratschbacher, L. The closure temperature(s) of zircon Raman dating. *Geochronology* **3**, 259–272 (2021).
32. Ewing R. C., Meldrum A., Wang L. M., Weber W. J., Corrales L. R. Radiation effects in zircon. *Rev. Mineral. Geochem.* **53**, 387–425 (2003).
33. Widmann, P., Davies, J. H. F. L. & Schaltegger, U. Calibrating chemical abrasion: Its effects on zircon crystal structure, chemical composition and UPb age. *Chem. Geol.* **511**, 1–10 (2019).
34. Svensen, H., Planke, S. & Corfu, F. Zircon dating ties NE Atlantic sill emplacement to initial Eocene global warming. *J. Geol. Soc.* **167**, 433–436 (2010).
35. Härtel, B. et al. Zircon Raman dating: age equation and calibration. *Chem. Geol.* **579**, 120351 (2021).
36. Kempe, U. et al. Substitution-induced internal strain and high disorder in weakly radiation damaged hydrothermal zircon from Mt. Malosa, Malawi. *Eur. J. Mineral.* **30**, 659–679 (2018).
37. Tapster, S., Roberts, N. M. W., Petterson, M. G., Saunders, A. D. & Naden, J. From continent to intra-oceanic arc: zircon xenocrysts record the crustal evolution of the Solomon island arc. *Geology* **42**, 1087–1090 (2014).
38. Rojas-Agramonte, Y. et al. Ancient xenocrystic zircon in young volcanic rocks of the southern Lesser Antilles island arc. *Lithos* **290-291**, 228–252 (2017).
39. Nasdala, L., Kostrovitsky, S., Kennedy, A. K., Zeug, M. & Esenkulova, S. A. Retention of radiation damage in zircon xenocrysts from kimberlites, Northern Yakutia. *Lithos* **206-207**, 252–261 (2014).
40. Hellebrand, E., Möller, A., Whitehouse, M. & Cannat, M. Formation of oceanic zircons. *Geochim. Cosmochim. Acta* **71**, A391–A391 (2007).
41. Grimes, C. B. et al. On the occurrence, trace element geochemistry, and crystallization history of zircon from in situ ocean lithosphere. *Contrib. Mineral. Petrol.* **158**, 757 (2009).
42. Chew, D. M., Petrus, J. A. & Kamber, B. S. U–Pb LA–ICPMS dating using accessory mineral standards with variable common Pb. *Chem. Geol.* **363**, 185–199 (2014).
43. Paton, C. et al. Improved laser ablation U-Pb zircon geochronology through robust downhole fractionation correction. *Geochem. Geophys. Geosyst.* (2010).
44. Wiedenbeck, M. et al. Three natural zircon standards for U-Th-Pb, Lu-Hf, trace element and ree analyses. *Geostand. Geoanal. Res.* **19**, 1–23 (1995).
45. Jackson, S. E., Pearson, N. J., Griffin, W. L. & Belousova, E. A. The application of laser ablation-inductively coupled plasma-mass spectrometry to in situ U–Pb zircon geochronology. *Chem. Geol.* **211**, 47–69 (2004).
46. Sláma, J. et al. Plešovice zircon—a new natural reference material for U–Pb and Hf isotopic microanalysis. *Chem. Geol.* **249**, 1–35 (2008).
47. Horstwood, M. S. A. et al. Community-derived standards for LA-ICP-MS U-(Th-)Pb geochronology—uncertainty propagation, age interpretation and data reporting. *Geostand. Geoanal. Res.* **40**, 311–332 (2016).
48. Vermeesch, P. IsoplotR: a free and open toolbox for geochronology. *Geosci. Front.* **9**, 1479–1493 (2018).
49. Wojdyr, M. Fityk: a general-purpose peak fitting program. *J. Appl. Crystallogr.* **43**, 1126–1128 (2010).
50. Váczi, T. A new, simple approximation for the deconvolution of instrumental broadening in spectroscopic band profiles. *Appl. Spectrosc.* **68**, 1274–1278 (2014).
51. Murakami, T., Chakoumakos, B. C., Ewing, R. C., Lumpkin, G. R. & Weber, W. J. Alpha-decay event damage in zircon. *Am. Mineral.* **76**, 1510–1532 (1991).
52. Pidgeon, R. T. Zircon radiation damage ages. *Chem. Geol.* **367**, 13–22 (2014).
53. Váczi, T. & Nasdala, L. Electron-beam-induced annealing of natural zircon: a Raman spectroscopic study. *Phys. Chem. Miner.* **44**, 389–401 (2017).
54. Jonckheere, R., Heinz, D., Hacker, B. R., Rafaja, D. & Ratschbacher, L. A borehole investigation of zircon radiation damage annealing. *Terra Nova* **31**, 263–270 (2019).
55. Hueck, M., Dunkl, I., Heller, B., Stipp Basei, M. A. & Siegesmund, S. (U-Th)/He thermochronology and zircon radiation damage in the South American passive margin: thermal overprint of the Paraná LIP? *Tectonics* **37**, 4068–4085 (2018).
56. Bjerga, A., Stubseid, H., Pedersen, L.-E. & Pedersen, R. B. Radiation damage allows identification of truly inherited zircon [Data set]. https://doi.org/10.5281/zenodo.5937936 (2022).

Acknowledgements

This work was funded by the K.G. Jebsen Foundation with support from the Norwegian Petroleum Directorate. The authors thank A. Beinlich for suggestions and comments on earlier drafts of this manuscript. We thank Fernando Bea, M. Francisco Pereira and the anonymous reviewers for constructive comments that helped to improve the quality of the manuscript. Thanks to Joe Aslin and João Duarte for their editorial management.

Author contributions

A.B. designed the study with input from H.H.S., L.E.R.P., and R.B.P. A.B. generated and interpreted the Raman data. L.E.R.P. generated geochronology data. R.B.P. secured funding for sample collection and analysis. A.B. wrote the paper with contributions from all co-authors.

Competing interests

The authors declare no competing interests.

Additional information

Supplementary information The online version contains supplementary material available at https://doi.org/10.1038/s43247-022-00372-2.

Correspondence and requests for materials should be addressed to Anders Bjerga.

Peer review information *Communications Earth & Environment* thanks Fernando Bea, M. Francisco Pereira and the other, anonymous, reviewer(s) for their contribution to the peer review of this work. Primary Handling Editors: João Duarte, Joe Aslin. Peer reviewer reports are available.

Reprints and permission information is available at http://www.nature.com/reprints

Publisher's note Springer Nature remains neutral with regard to jurisdictional claims in published maps and institutional affiliations.